Enhanced Isotope Discrimination Using Electromagnetically Induced Transparency

A. Kasapi*
Edward L. Ginzton Laboratory, Stanford University, Stanford, California 94305
(Received 14 March 1996)

Electromagnetically induced transparency is applied to isotope discrimination. By adjusting the intensity of a coupling laser, one isotope is made resonantly opaque while another is rendered transparent to a probe. Experimental results are shown in isotopically enriched atomic lead, where 0.03% ^{207}Pb is clearly seen against a background of ^{208}Pb. [S0031-9007(96)00813-7]

PACS numbers: 42.50.Gy, 31.30.Gs, 32.80.–t, 42.50.Hz

In this Letter, a new laser-based technique to discriminate between two isotopes of the same element is suggested and experimentally demonstrated. Briefly, one of the isotopes is rendered highly opaque while the other is simultaneously rendered highly transparent, allowing a trace amount of one isotope to be detected against the background of a far more prevalent isotope. The technique is demonstrated in isotopically enriched atomic lead comprised of 99.97% ^{208}Pb and 0.03% ^{207}Pb, showing a clear signal from ^{207}Pb against the large background of ^{208}Pb. While the technique is demonstrated with photoabsorption, it can alternatively be combined with other isotope discrimination methods such as laser photoionization spectroscopy and resonance ionization spectroscopy [1].

This work follows from recent work studying electromagnetically induced transparency (EIT) in atomic media where a single species is rendered maximally transparent [2] and highly dispersive [3–6]. Certain analogies exist as well to recent work in nonlinear optics [7] and lasers without inversion [8].

The prototypical atomic system under consideration has three states [Fig. 1(a)]: a ground state $|1\rangle$, an upper state $|3\rangle$ (forming a dipole allowed transition with the ground state), and an auxiliary state $|2\rangle$. The homogeneous FWHM linewidth of the $|1\rangle \rightarrow |2\rangle$ transition is $2\gamma_2$ and that of the $|1\rangle \rightarrow |3\rangle$ transition is $2\gamma_3$. Two fields are applied: a monochromatic "coupling" field given by $\mathcal{E}_c = \exp(i\omega_c t)$ and a "probe" field given by $\mathcal{E}_p = \exp(i\omega_p t)$. The coupling field is tuned near the $|2\rangle \rightarrow |3\rangle$ transition and has detuning $\Delta\omega_c = \omega_{32} - \omega_c$ and the probe field is tuned near the $|1\rangle \rightarrow |3\rangle$ transition with detuning $\Delta\omega_p = \omega_{31} - \omega_p$ (Fig. 2). The expression for the susceptibility seen by the probe is

$$\chi(\omega_p) = \frac{|\mu_{13}|^2 N}{\epsilon_0 \hbar}\left(\frac{\Delta\tilde{\omega}_2}{\Delta\tilde{\omega}_2\Delta\tilde{\omega}_3 - |\Omega_c|^2/4}\right), \quad (1)$$

where μ_{13} is the relevant matrix element of the $|1\rangle \rightarrow |3\rangle$ transition, $\Omega_c = \mu_{23}\mathcal{E}_c/\hbar$ is the Rabi frequency of the coupling laser on the $|2\rangle \rightarrow |3\rangle$ transition (and μ_{23} is the relevant matrix element), N is the atom density, $\Delta\tilde{\omega}_2 = (\Delta\omega_p - \Delta\omega_c) + i\gamma_2$, and $\Delta\tilde{\omega}_3 = \Delta\omega_p + i\gamma_3$.

The new technique can be understood by considering two isotopes, A and B, exhibiting slightly different spectra, so that in isotope B both the $|2\rangle \rightarrow |3\rangle$ and $|1\rangle \rightarrow |3\rangle$ transitions are of higher energy. The susceptibility seen by isotope A is examined first. As shown in Fig. 1(a), the laser frequencies are chosen to be resonant ($\Delta\omega_p = \Delta\omega_c = 0$) and Ω_c is sufficiently large [9] that the susceptibility is well approximated by

$$\chi(\omega_p)A = -i\frac{|\mu_{13}|^2 N}{\epsilon_0 \hbar}\frac{4\gamma_2}{|\Omega_c|^2}. \quad (2)$$

When the coupling laser is omitted ($\Omega_c = 0$) so that $|2\rangle$ is no longer coupled to the probe, the susceptibility is

$$\chi(\omega_p) = \frac{|\mu_{13}|^2 N}{\epsilon_0 \hbar}\left[\frac{\Delta\omega_p - i\gamma_3}{\gamma_3^2 + \Delta\omega_p^2}\right], \quad (3)$$

whose imaginary part has the same form as Eq. (2), with the correspondence $\Delta\omega_p \leftrightarrow \Omega_c/2$ and $\gamma_2 \leftrightarrow \gamma_3$.

The first correspondence is not surprising: The coupling laser ac Stark splits the state $|3\rangle$ into a pair of "dressed" states separated by the Rabi frequency Ω_c [Fig. 1(b)] so that the probe, tuned near state $|3\rangle$, is detuned from the states of the dressed atomic system by $\Omega_c/2$. The second correspondence is more subtle; whereas one may have expected the upper-state linewidth

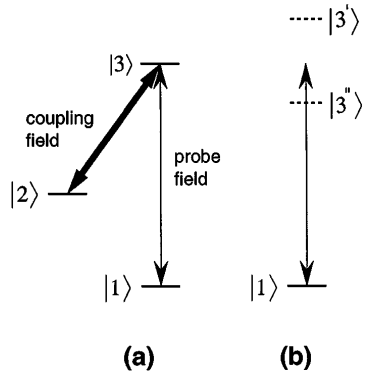

FIG. 1. Prototypical three-state system with lasers tuned near resonance. (a) State $|1\rangle$ is the "ground state," state $|2\rangle$ is a "metastable state," and state $|3\rangle$ is a state with dipole-allowed transitions to $|1\rangle$ and $|2\rangle$. A strong coupling field tuned near the $|2\rangle \rightarrow |3\rangle$ transition is applied and a probe field is tuned near the $|1\rangle \rightarrow |3\rangle$ transition. (b) The coupling field is tuned exactly onto the $|2\rangle \rightarrow |3\rangle$ transition; the probe sees "dressed states" $|3'\rangle$ and $|3''\rangle$ separated by the coupling Rabi frequency Ω_c.

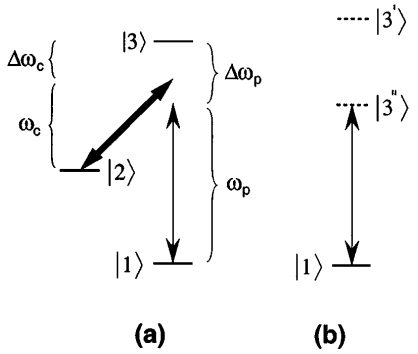

FIG. 2. Isotope B with lasers tuned to resonance with the transitions of isotope A. (a) The fields are detuned from the isotope B transitions; the probe and coupling laser radian frequencies are ω_p and ω_c, respectively, and the detunings are $\Delta\omega_p$ and $\Delta\omega_c$ (both shown positive). (b) For the correct coupling field strength dressed state $|3''\rangle$ moves into resonance with the probe.

γ_3 to appear, γ_2 appears instead. As a consequence, since $\gamma_2 \ll \gamma_3$, the medium is far less absorbing—it has been rendered "transparent."

The susceptibility seen by isotope B is now examined. For lasers tuned to the transitions of A, $\Delta\omega_p$ and $\Delta\omega_c$ are now nonzero, as shown in Fig. 2(a), and the transparency is reduced. One can therefore discriminate between two atomic species based on this difference in transparency. It is in fact possible to carry this reasoning one step further by rendering A transparent and simultaneously rendering B maximally opaque. To see this, note that for $\Omega_c \approx 2\sqrt{\Delta\omega_p(\Delta\omega_p - \Delta\omega_c)}$, the denominator of Eq. (1) becomes very small and there is a resonant enhancement in the susceptibility. This result presupposes that the one-photon detuning $\Delta\omega_p$ and the two-photon detuning $\Delta\omega_p - \Delta\omega_c$ have the same sign, but that is all.

The interpretation of this result is shown in Fig. 2(b). The probe laser is weak and the coupling laser is much stronger, and the effect of the coupling laser on the upper state $|3\rangle$ as it is probed by the weak probe laser is considered. According to standard theory [10], apparent dressed states, shown as $|3'\rangle$ and $|3''\rangle$, appear. As Ω_c is increased, the two states $|3'\rangle$ and $|3''\rangle$ move apart; for the detunings shown in Fig. 2(a), state $|3'\rangle$ moves up and state $|3''\rangle$ moves down. In the present situation, where the probe is tuned to the resonance transition of isotope A, for the correct Ω_c, state $|3''\rangle$ moves onto resonance with the probe at ω_p and thus a condition of maximal interaction between the atom and the field is realized.

In principle, this procedure can be used for any pair of isotopes, although practical considerations restrict its applicability. Atoms in typical media have inhomogeneously broadened transitions so that it is impossible to achieve $\Delta\omega_p = \Delta\omega_c = 0$ for every atom of the transparent species. Denoting the inhomogeneous linewidth (FWHM) of the $|1\rangle \rightarrow |2\rangle$ transition by $\Delta\omega_{D2}$ and that of the $|1\rangle \rightarrow |3\rangle$ transition by $\Delta\omega_{D3}$, then the condition for transparency is

$$|\Omega_c|^2 \gg \max[4\gamma_2\gamma_3, \Delta\omega_{D2}\Delta\omega_{D3}, (\gamma_3/\gamma_2)\Delta\omega_{D2}^2]. \quad (4)$$

This condition restricts the candidate isotope detunings $|\Delta\omega_p|, |\Delta\omega_c|$ to exceed $\max(2\sqrt{\gamma_2\gamma_3}, \sqrt{\Delta\omega_{D2}\Delta\omega_{D3}}, \Delta\omega_{D2}\sqrt{\gamma_3/\gamma_2})$ [9].

If either isotope exhibits hyperfine splitting, the analysis becomes more complex but the principle is unchanged: One isotope is rendered transparent and, simultaneously, Ω_c is adjusted until, in the other isotope, a dressed state is ac Stark shifted into resonance with the probe so that it interacts strongly with the field.

Consider now two isotopes of gas-phase atomic lead, ^{208}Pb and ^{207}Pb. An energy-level diagram (not to scale) of the isotopes following [11] is shown in Fig. 3. In ^{208}Pb, state $|3\rangle$ is the upper state of the resonance transition, state $|1\rangle$ is the ground state, and state $|2\rangle$ is a metastable state since there are no opposite-parity states of lower energy. Conditions are assumed for which both the $|1\rangle \rightarrow |3\rangle$ and $|1\rangle \rightarrow |2\rangle$ transitions are collisionally broadened and that $\gamma_2 < \gamma_3$.

In ^{207}Pb, states $|2\rangle$ and $|3\rangle$ are split by a hyperfine interaction. Both lasers are tuned onto resonance with the ^{208}Pb transitions, and their detunings from the ^{207}Pb transitions are as indicated by the arrows in Fig. 3.

It is reasonable to expect that there exists some Ω_c (with respect to the ^{208}Pb $|2\rangle \rightarrow |3\rangle$ transition) for which some state in ^{207}Pb is ac Stark shifted into resonance with the probe field. To verify this, the imaginary (absorptive) part of the susceptibility for ^{207}Pb at the probe frequency is calculated as a function of Ω_c. The results are shown in Fig. 4. The parameters used in the calculations are as reported in [5,12]; no Doppler broadening is included in the calculation. There is an absorptive resonance at $\Omega_c = 0.45$ cm^{-1}. Taking Doppler broadening into account (at a temperature of 800 °C), the absorptive cross

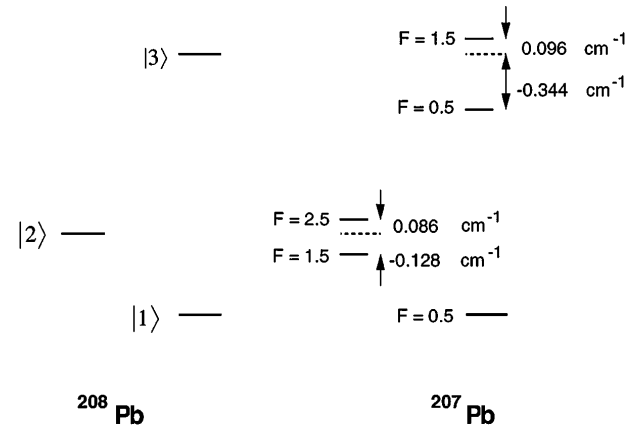

FIG. 3. Energy level diagrams of ^{208}Pb and ^{207}Pb (not drawn to scale). States $|1\rangle$, $|2\rangle$, and $|3\rangle$ denote the states $6s^2 6p^2\,{}^3P_0$ (ground), $6s^2 6p^2\,{}^3P_2$ (metastable at 10 650 cm^{-1}, and $6s^2 6p 7s\,{}^3P_1$ (at 35 287 cm^{-1}), respectively. In ^{207}Pb, states $|2\rangle$ and $|3\rangle$ are split by the hyperfine interaction and are separated from the unsplit ^{208}Pb states as shown.

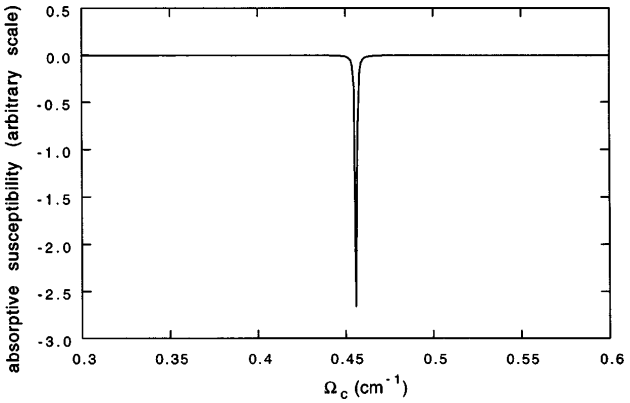

FIG. 4. Calculation of the imaginary (absorptive) portion of the ^{207}Pb susceptibility as a function of Ω_c. Both the coupling and probe lasers are tuned onto resonance with the ^{208}Pb transitions. Inhomogeneous broadening is not included in the calculation. An absorptive resonance is seen at $\Omega_c = 0.45$ cm^{-1}.

section seen by the probe for this resonant Ω_c in ^{207}Pb and ^{208}Pb is $3.2 \times 10^{-13}/\text{cm}^2$ and $2.4 \times 10^{-17}/\text{cm}^2$, respectively, so that the ratio of the cross sections is 1.3×10^4.

In order to place EIT enhanced isotope discrimination in perspective, consider the simplest alternative discrimination method: No coupling laser is used and the probe laser is simply tuned onto resonance with the strongest ^{207}Pb resonance transition ($\Delta\omega_p = -0.344$ cm^{-1}); with Doppler broadening taken into account as above, the absorption cross section for the probe is then 4.4×10^{-13} cm^2. The absorption cross section due to ^{208}Pb atoms is 2.6×10^{-16} cm^2, so that the ratio in the cross sections is 1.7×10^3. This ratio is the figure of merit for isotope discrimination, and it is approximately an order of magnitude higher in the EIT scheme.

The remainder of this Letter describes an experimental demonstration using isotopically enriched atomic lead comprised of 99.97% ^{208}Pb and 0.030% ^{207}Pb [13]. The apparatus is described more fully elsewhere [5] and will be only briefly outlined here. The lead is contained in a 10 cm-long sealed quartz side-arm cell heated to in excess of 800 °C to produce a lead density of 1×10^{15} atoms/cm^3. The 406 and 283 nm probe and coupling lasers, which copropagate through the cell, are produced by harmonic mixing from seeded, single-longitudinal-mode pulsed Ti:sapphire lasers [14].

The probe and coupling beams have opposite circular polarization and are focused into the center of the cell with beam diameters (measured to the $1/e$ points) of 0.2 and 0.9 mm, respectively. The probe beam is centered on the spatially uniform central portion of the larger coupling laser beam and remains centered for the length of the cell. The relative timing of the two lasers is adjusted so that the coupling laser enters the cell before the probe and is present until after the probe has left the cell. Fast photodetectors are connected to a 5×10^9 sample/s Tektronix TDS 684A four-channel, real-time digital oscilloscope to simultaneously record the probe and coupling laser pulse wave forms before (via beam splitters) and after they exit the cell. The oscilloscope wave forms are periodically transferred to a computer, where they are recorded. All data points shown in this Letter are from individual pulses and are not averaged.

The voltage signal of the coupling laser detector is calibrated to the coupling laser Rabi frequency (Ω_c) by fixing the coupling laser power and scanning the probe laser frequency to determine the Autler-Townes splitting of state $|3\rangle$. For good frequency resolution this is done in a relatively optically thin cell. The probe laser intensity is kept much lower than the saturation intensity of the $|1\rangle \rightarrow |3\rangle$ transition.

Figure 5 shows the probe transmission vs $\Delta\omega_p$ with $\Omega_c = 0$. Because of the limited signal-to-noise ratio of the data inherent in this kind of pulsed-laser experiment, an extra dip at 0.096 or -0.344 cm^{-1}, indicating the presence of ^{207}Pb, cannot be seen. From this plot, and using the $|1\rangle \rightarrow |3\rangle$ transition linewidth measured using the method described in [9], the ^{208}Pb atom density is $N = 1 \times 10^{15}$ atoms/cm^3.

Figure 6 shows the result when the coupling laser is allowed into the cell; the probe transmission is plotted as a function of the peak Ω_c (only shots where the coupling laser peak occurs near the probe laser peak are retained). The absorption peak from ^{207}Pb shown in Fig. 4 appears in the data at $\Omega_c \approx 0.41$ cm^{-1}, close to its predicted location.

The expected depth of the dip is the product of the ^{207}Pb absorption cross section, the ^{207}Pb atom density, and the cell length. For the conditions of this experiment, this is -1. The plot shows a dip of approximately 0.5, which is in reasonable agreement given the pulse-to-pulse frequency, amplitude, and pointing jitter of the lasers.

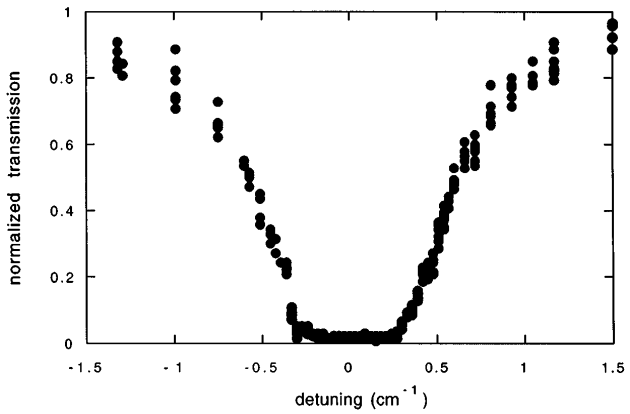

FIG. 5. Probe transmission vs probe frequency in the cell containing 99.97% ^{208}Pb and 0.03% ^{207}Pb. There is no indication of the presence of ^{207}Pb. The atom density is 1×10^{15} atoms/cm^3, determined as in Ref. [8].

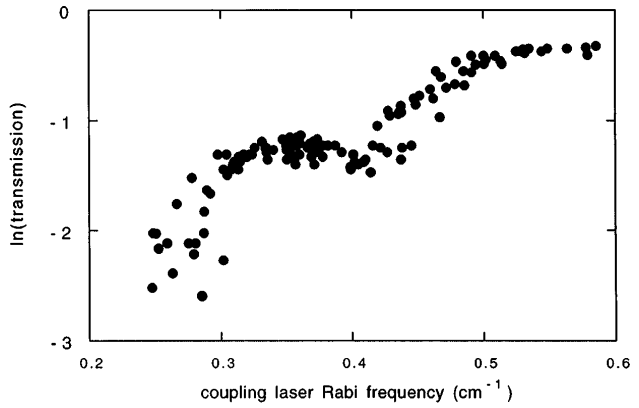

FIG. 6. Probe transmission vs coupling laser Rabi frequency with the probe tuned onto resonance with the $|1\rangle \rightarrow |3\rangle$ transition in ^{208}Pb. An absorption dip appears near its predicted location; the depth of the dip is 0.5, and it is within a factor of 2 of the predicted depth of -1.

In conclusion, a new technique to discriminate between atomic isotopes is proposed and demonstrated. This technique, using two lasers, exploits EIT in one isotope and ac Stark shifting in the other to provide significantly stronger discrimination signals compared to the signals obtained with only one tuned laser. This is one example where EIT, by making a dominant species transparent, allows one to see a hidden species. While isotope discrimination is the specific case discussed here, this concept can be generalized to discriminate between any pair of species whose states are slightly displaced or split with respect to each other.

The author gratefully acknowledges contributions by M. Jain, G. Y. Yin, and helpful discussions with S. E. Harris. This work was supported by the U.S. Office of Naval Research, the U.S. Army Research Office, and the U.S. Air Force Office of Scientific Research.

*Present address: ArrayComm, Inc., San Jose, CA 95134.

[1] V. S. Letokhov, *Laser Photoionization Spectroscopy* (Academic Press Inc., New York, 1987); G. S. Hurst, *Principles and Applications of Resonance Ionisation Spectroscopy* (Adam Hilger, Bristol, United Kingdom, 1988);W. M. Fairbank, Jr., M. T. Spaar, J. E. Parks, and J. M. R. Hutchinson, Phys. Rev. A **40**, 2195 (1989).

[2] K. J. Boller, A. Imamoglu, and S. E. Harris, Phys. Rev. Lett. **66**, 2593 (1991); J. E. Field, K. H. Hahn, and S. E. Harris, Phys. Rev. Lett. **67**, 3062 (1991).

[3] S. E. Harris, J. E. Field, and A. Kasapi, Phys. Rev. A **46**, R29 (1992).

[4] M. Xiao, Y.-Q. Li, S.-Z. Jin, and J. Gea-Banacloche, Phys. Rev. Lett. **74**, 666 (1995).

[5] A. Kasapi, M. Jain, G. Y. Yin, and S. E. Harris, Phys. Rev. Lett. **74**, 2447 (1995).

[6] S. E. Harris, Opt. Lett. **19**, 2018 (1994).

[7] K. Hakuta, L. Marmet, and B. P. Stoicheff, Phys. Rev. A **45**, 5152 (1992); S. P. Tewari and G. S. Agarwal, Phys. Rev. Lett. **56**, 1811 (1986); S. E. Harris, J. E. Field, and A. Imamoglu, Phys. Rev. Lett. **64**, 1107 (1990); M. Jain, G. Y. Yin, J. E. Field, and S. E. Harris, Opt. Lett. **18**, 998 (1993).

[8] Marlan O. Scully, Quantum Opt. **6**, 203 (1994), and references therein; O. Kocharaovskaya and P. Mandel, Quantum Opt. **6**, 217 (1994).

[9] A. Kasapi, G. Y. Yin, M. Jain, and S. E. Harris, Phys. Rev. A **53**, 4547 (1996).

[10] C. Cohen-Tannoudji, J. Dupont-Roc, and G. Grynberg, *Atom-Photon Interactions* (John Wiley & Sons, Inc., New York, 1982).

[11] J. Murakawa, J. Phys. Soc. Jpn. **8**, 382 (1953); M. J.-L. Cojan and H. R. Saussereau, C.R. Acad. Sci. Ser. Gen. Ser. B **277**, 415 (1973); T. E. Manning, C. E. Anderson, and W. W. Watson, Phys. Rev. **78**, 417 (1950).

[12] R. L. DeZafra and A. Marshall, Phys. Rev. **170**, 128 (1968).

[13] Oak Ridge National Laboratory, Oak Ridge, Tennessee.

[14] G. Y. Yin, A. Kasapi, M. Jain, and A. Merriam, in *Conference on Laser and Electro-Optics*, 1994 OSA Technical Digest Series Vol. 8 (Optical Society of America, Washington, DC, 1994), p. 118; A. Kasapi, G. Y. Yin, and M. Jain, Appl. Opt. **35**, 1999 (1996); T. D. Raymond, Opt. Lett. **16**, 33 (1991).